International Journal of
Numerical Modelling
Electronic Networks, Devices and Fields

The Impact of Pore Diameters, Pore Randomness, and Void Fraction on the EMI Shielding of Polyurethane Foams

Journal:	*International Journal of Numerical Modelling: Electronic Networks, Devices and Fields*
Manuscript ID	JNM-25-0066.R2
Wiley - Manuscript type:	Research Article
Date Submitted by the Author:	18-Aug-2025
Complete List of Authors:	Khamis, Ahmad Mamoun; Universite Catholique de Louvain Institute of Information and Communication Technologies Electronics and Applied Mathematics Huynen, Isabelle; Universite Catholique de Louvain Institute of Information and Communication Technologies Electronics and Applied Mathematics
Keywords:	CST Studio software, electromagnetic interference, polyurethane foam, EMI shielding, absorption

SCHOLARONE™
Manuscripts

The Impact of Pore Diameters, Pore Randomness, and Void Fraction on the EMI Shielding of Polyurethane Foams

Ahmad Mamoun Khamis[1*] and Isabelle Huynen[1]

[1] ICTEAM Institute, Université Catholique de Louvain, Louvain-la-Neuve, 1348 Belgium, (e-mail: isabelle.huynen@uclouvain.be).

[*] Corresponding author: Ahmad.khamis@uclouvain.be.

ABSTRACT

This paper presents a novel approach to analyze the electromagnetic interference (EMI) shielding effectiveness (SE) of polyurethane (PU) foam geometries, which are built in Blender software, and simulated using CST Studio software. Three different batches of geometries were built to investigate the impact of void fraction, pore diameters, and pore randomness of PU foam on the SE, reflection coefficient (S_{11}) and electromagnetic absorption in the 26.5 – 40 GHz frequency range. The observed resonance frequency decreased with decreasing pore diameters and void fraction. Decreasing the pore diameter, increasing the pore randomness, and decreasing the void fraction enhanced the SE in the frequency range between the resonance frequency and 40 GHz. The EM absorption increased with increasing the pore diameter and randomness but decreased with increasing the void fraction. This study also presents simulations and measurements of Polytetrafluoroethylene (PTFE) and PU foam materials. The simulation results were compared with the measured ones obtained using vector network analyzer measurements, to verify CST Studio's ability to accurately calculate the EM parameters. The measured and simulated results were in good agreement, confirming the accuracy of the results obtained using CST Studio. Our new parametric study fills a gap in existing literature since it combines for the first time an open-source 3D software for 3D rendering with an electromagnetic simulator to evaluate the impact of the pore topography (void fraction, diameter, randomness, etc) on the EMI shielding performance of PU foams.

KEYWORDS

CST Studio software, electromagnetic interference, polyurethane foam, pore diameters, pore randomness, void fraction, EMI shielding, absorption, microwaves.

I. INTRODUCTION

The electromagnetic interference in the microwave and radio frequency range is a huge challenge for modern society. However, the negative impact of the EMI can be decreased by placing a shielding material between the sensitive component and the electromagnetic (EM) source [1]. Improving the EM reflection, absorption, and multireflection of a microwave signal can enhance the EMI shielding performance. Metals are used as EMI shielding materials due to their high conductivity; however, their corrosive nature and heavy weight are disadvantages [2, 3]. Therefore, polymer-based composites are a popular choice for EMI shielding applications due to their high strength, low cost, simple processing, lightweight, resistance to corrosion and degradation [4]. For example, different commercial polymers such as polyurethane are used as base polymers

For Peer Review

[5]. In addition, the polymer foam has many advantages that meet the requirements of EMI shielding applications such as the lightweight and porous structure that can effectively attenuate the EM signals by prolonging the travel path [3]. PU foam is used in a wide range of applications such as insulators, high-efficiency coatings, advanced controllers, and EMI shielding applications [6]. Many studies investigated the impact of conductive fillers on the PU foam matrix for EMI shielding applications, such as Fe_3O_4 and silver [7], graphite [8], graphene, reduced graphene oxide [9], multiwall carbon nanotube (MWCNT) [10], and nickel-coated carbon fiber [11]. Therefore, investigating the EMI shielding properties of PU foam matrix is crucial for enhancing the shielding performance of PU foam composites.

A growing body of research focused on the impact of void fraction (VF) and pore diameter on the EMI shielding properties using experimental methods. For example, Zhao et al. experimentally studied the effects of VF in the poly(vinylidene fluoride) (PVDF)/ MWCNT composite foams [12] while Wu et al. investigated the impact of cell size in polypropylene/carbon nanostructure (PP/CNS) nanocomposite foams [13] on the EMI shielding properties. The impact of pore structure on the EMI shielding properties of carbonized wood was also investigated [14]. Our work investigates the impact of VF and cell size of PU foam on EMI shielding properties using a theoretical approach.

Recently, researchers have started to consider using computational-based approaches to develop composite foams for EMI shielding [15], improve the understanding of the relationship between structure, properties, and process of foams [16]. In [15], a theoretical computation approach was used to demonstrate the best results for layered PVDF-based composite foams consisting of SiC nanowires, MXene nanosheets, and CNT. In [17], the relationship between the void fraction and the electrical percolation threshold was experimentally and theoretically investigated using a modified Monte Carlo model. In [18], the effects of cell density and void fraction of PVDF/ CNT/SiC nanowire (SiCnw) composite foams on the EMI shielding were also theoretically evaluated by an input impedance model and then experimentally validated. In [19], the RF model in COMSOL Multiphysics was used to simulate PU foam geometries built using a computer-aided design (CAD) Kernel. In [20], the SE performance of Teflon carbon filled composite shielding enclosures was studied using a genetic algorithm optimization GA in the 100 MHz – 10 GHz frequency range. Additionally, the FDTD (finite difference time-domain) simulation was used to situate the SE of a composite layer box at 10 – 50 dB.

A new approach to build PU foam geometries using Blender software will be introduced in this study. Blender is free and open-source software for 3D rendering. It supports all kinds of 3D-related work such as simulation, animation, modeling, video editing, and compositing [21]. Recent research conducted in 2024 and 2025 shows that Blender software was used to design a CAD model of honeycomb structures for EMI shielding [22, 23]. The absence of relevant studies on foam geometries built using Blender software and simulated using CST Studio for EMI shielding applications reflects the importance of this study and motivates our approach.

It is also worth noting that limited research focused on the impact of pore randomness on the EMI shielding properties. Random porous structures were modeled using different software for different purposes, such as Surface Evolver for compressive deformation [24], CAD model for laser powder bed fusion [25], smoothed particle hydrodynamics (SPH) method for fracture mechanical properties [26], and Python for mechanical properties [27]. Minas et al. also studied the effects of pore randomness on effective mass diffusivity [28]. Additionally, the impact of oriented and random porous structures of poly (vinyl alcohol) (PVA) on EMI shielding performance was investigated by Wang et al [29]. However, the impact of increasing the pore randomness of PU foam on the EMI shielding properties and resonance frequency has not yet been reported. Investigating the resonance frequency is important in EMI shielding applications because it corresponds to a maximum of absorption, which in turn induces a local maximum of EMI. This local maximum can be useful when narrowband selective shielding is desired.

In our study, we aim to address this gap in the literature. The Voronoi node in Blender Software can be

For Peer Review

used to generate random pore patterns, which can be tuned to build different structures by varying the resulting randomness [30]. Our research investigates the effects of increasing the pore randomness of PU foam on EMI shielding properties and resonance frequency using CST Studio.

CST Studio Suite® is a high-performance 3D EM analysis software package for designing, analyzing, and optimizing electromagnetic components and systems. The CST Studio was used to predict the gain performance of a wide variety of millimeter-wave metamaterial foam structures in the 50 – 70 GHz frequency range [31]. It was also used to simulate the reflectivity of a flexible microwave-absorbing foam material based on the dielectric properties [32], the electric field vector distribution on the upper surface of a 3D porous foam model and electric field distribution at 10 GHz [33]. The reflectivity and transmissivity of composite material based on indium tin oxide film metamaterial were simulated using CST Studio [34]. The shielding effectiveness of a double wire-mesh screen (metal foam) was also calculated using CST, however, the meshes were assumed to be square [35]. The EMI shielding of layered flexible films of poly(ethylene terephthalate), carbon nanofibers (CNFs), and polyurethane was analyzed using the same software in the 1 – 18 GHz frequency range [36]. The frequency selective surface reflection coefficient for electromagnetic shielding was analyzed in the 4 – 22 GHz frequency range using CST software [37]. Furthermore, it was used to calculate the shielding effectiveness of the shielding cabinet in the radio observatory site in the 0.1 – 3 GHz frequency range [38].

In recent years, there was a significant increase in studies that focused on using CST Studio to simulate various foam geometries, such as ceramic [39], aluminum [40], polyurethane [41], silicone [42], and polydimethylsiloxane [32] for different microwave applications including EMI shielding. Such a rapid surge of studies last year highlights the necessity of simulating PU foam geometries, built using Blender software, using CST studio because none of the previous studies used Blender software to build PU geometries.

In this research, three different batches of geometries were built using Blender software to study the impact of void fraction, pore diameters, and pore randomness on the shielding properties of PU foam in the 26.5 – 40 GHz frequency range. The purpose of this study is to investigate the effects of the aforementioned parameters on EMI shielding properties, paving the way to produce materials with high EMI shielding performance. Therefore, pure PU foam, without any conductive fillers such as carbon nanotubes (CNTs), was investigated in this research. The Ka-band frequency range was chosen for this study because it will be widely used for high data-rate communication in the 5G new radio [43]. The applications of this frequency range involve two-way broadband internet, remote area communications, mobile backhaul, very small aperture terminal (VSAT) systems, disaster management, satellite news gathering, enterprise applications, and defense applications [44].

II. Modeling and Simulation Procedures

The surface dimensions of the PU foam geometry were 7.112 mm x 3.556 mm, and they were chosen based on the standard rectangular waveguide size of WR28 [45]. The thickness of the PU foam geometry was 3 mm. Blender 4.1 software was used to construct the PU foam geometries exported in the STL format for inclusion in the CST Studio environment. The input values for the PU material were as follows: dielectric constant was 6.55 and the loss tangent was 0.026 [46]. Three different batches of geometries were constructed as follows: variation of pore diameter (Section II.A), variation of pore randomness (Section II.B), and variation of void fraction (Section II.C).

A. Pore Diameters

Four different geometries of PU foam were constructed based on different pore diameters, noted d. The average diameters of the geometries were as follows: d = 0.47 mm, d = 0.57 mm, d = 0.67, and d = 0.9. The average value of measured pore diameters of PU foam was 0.46 mm as described in Section III.D. Therefore, the pore diameter of 0.47 mm was selected based on the ± 0.01 mm range of the measured value. The values

of 0.57 mm and 0.67 mm were chosen based on a 0.1 mm increment pattern. The value of 0.9 was chosen as a high value to investigate if the EMI shielding will continue to change gradually, or if a drastic change will take place at 0.9 mm geometry. The void fraction (VF) and pore randomness were maintained constant in this study. The VF was 0.72 while the pore randomness factor was 0.2. The plan view of each geometry in the pore diameters study is presented in Fig. 1.

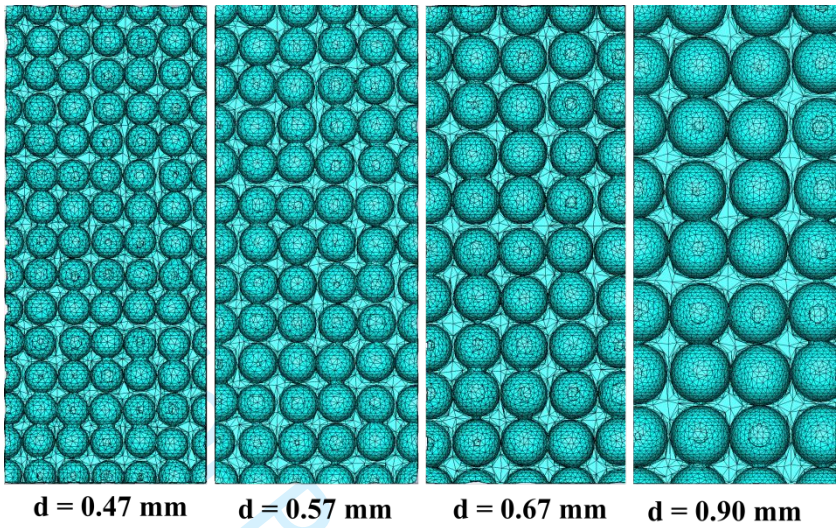


Fig. 1. Plan view for PU geometries in the pore diameters study.

B. Pore Randomness

This study investigated the effects of pore randomness of PU foam on the EMI shielding properties. Eight geometries with different randomness factors noted R were built using Blender software as presented in Fig. 2. The tool of Voronoi Texture node was used to manipulate the pore's randomness. This tool is preferred because it can show comparable randomness [30]. The R values used in this study were as follows: 0, 0.1, 0.2, 0.3, 0.4, 0.5, 0.6 and 0.7. These values were selected based on the available range of randomness in Blender Software. The pore's randomness increased with increasing R. The VF was 0.72 while the average d was 0.9 mm.

Peer Review

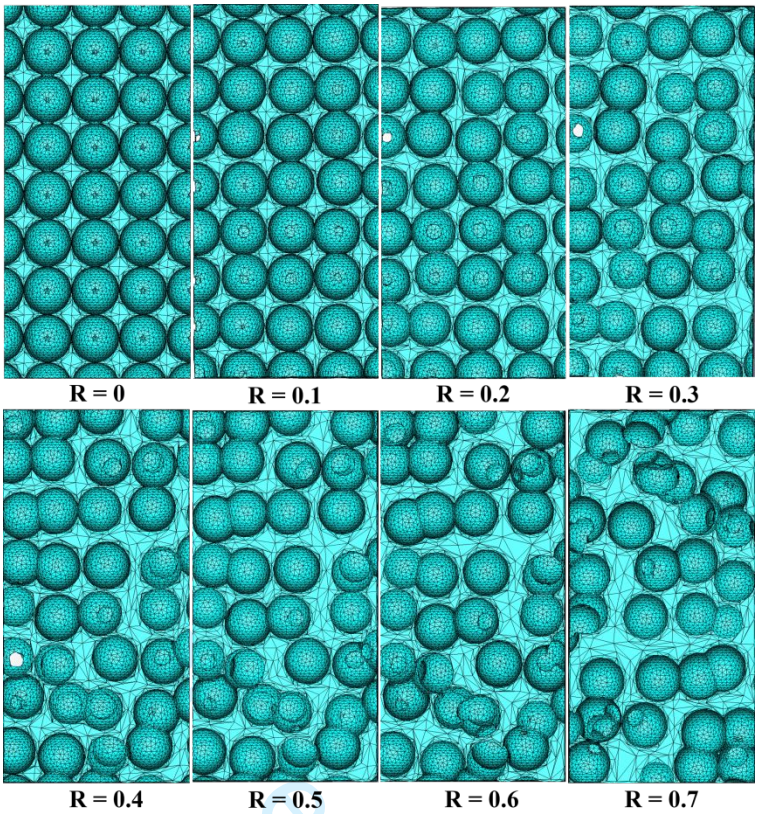


Fig. 2. Plan view for PU geometries in the pore randomness study.

C. Void Fraction

Eight geometries with different VF were constructed as presented in Fig. 3. The VF of PU geometries was calculated as the ratio of the void area to the total surface area [47]. The VF values are always between 0 and 1. [48]. Therefore, the VF values investigated in this article were 0, 0.50, 0.56, 0.61, 0.70, 0.75, 0.79, and 0.90. Such values cover a wide range of VF for PU. ImageJ 1.53e (image processing program) was used to measure the area of the pores and the total surface area. The average d of this study was 0.9 mm while R was 0.7.

Peer Review

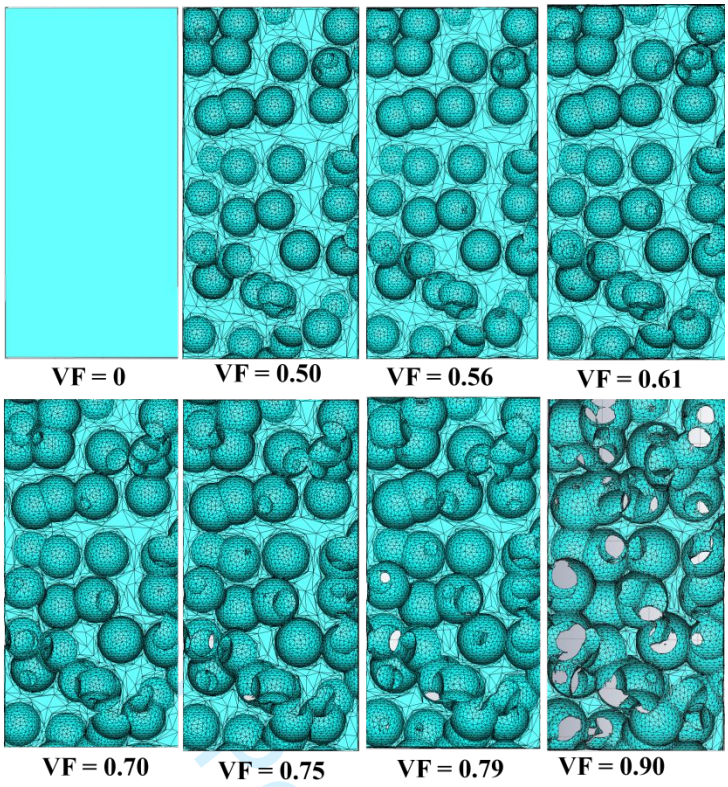


Fig. 3. Plan view for PU geometries in the VF study.

The PU geometries exported from Blender software in the STL format were then imported and simulated in CST Studio. The transmission coefficient (S_{21}) and reflection coefficient (S_{11}) were obtained from CST simulation and used to compute the absorption coefficient (A) using the following formula [49]:

$$A = 1 - |S_{11}|^2 - |S_{21}|^2 \quad (1)$$

The SE (dB) [50, 51] and S_{11} (dB) [52] were calculated using the following formulas:

$$SE\ (dB) = SE_A + SE_R \quad (2)$$

$$SE(dB) = -10log_{10}\frac{|S_{21}|^2}{1-|S_{11}|^2} - 10log_{10}(1-|S_{11}|^2) \quad (3)$$

$$SE\ (dB) = -\ 20.log_{10}\ (S_{21}) \quad (4)$$

$$S_{11}\ (dB) = 20.log_{10}\ (S_{11}) \quad (5)$$

III. RESULTS

A. Pore Diameters

Increasing the diameter of the pore significantly impacted the SE (dB), S_{11} (dB), and EM absorption of PU foam geometries as shown in Figs. 4, 5, and 6, respectively. The four geometries exhibited resonance frequencies as listed in Table I. The fr values were identified based on the minimum points (dips) in S_{11} (dB) curves. Fig. 7 shows that increasing the diameter of pores in PU foam caused an increase in resonance frequency. The SE decrement in geometries with larger pore diameters, associated with higher EM

transmission, could be attributed to the fact that the EM waves experienced less interaction with pore walls in larger pores compared to smaller ones as shown in Fig. 8. Some EM waves perpendicularly hit the pores wall and continue their path without any refractions, based on Snell's law, because the angle between the normal and the EM wave is zero. Such waves interact with the pore walls three times in the 0.9 mm geometry, whereas in the 0.46 mm geometry, they interact six times.

In addition, the geometries with pore diameters of 0.9 mm and 0.67 mm exhibited another resonance frequency at 34.84 GHz and 34.56 GHz, respectively. The reason for these two resonance frequencies could be attributed to the high EM absorption as presented in Fig. 6. In geometries with larger pore diameters, the EM waves travel longer distances, compared to geometries with smaller pores, inside the pores before hitting the pore walls and reflecting. Such behavior could lead to higher EM absorption for certain wavelengths. The SE increased with increasing the diameter of the pores until reaching the resonance frequency where the opposite behavior was experienced.

The empirical equation and correlation coefficient (R^2) which link the pore's diameter and resonance frequency were calculated using Microsoft Excel based on the four datasets presented in Fig. 7. The empirical equation is expressed as follows:

$$fr = 2.6592.d + 27.977 \quad (6)$$

The R^2 value is 0.98 which indicates that d and fr have a strong positive relationship because the value of R^2 is close to one [6]. Therefore, the value of fr, can be predicted using this equation at a specific pore's diameter. For instance, the fr of PU foam geometry with 0.8 mm pore diameter is expected to be 30.10 GHz.

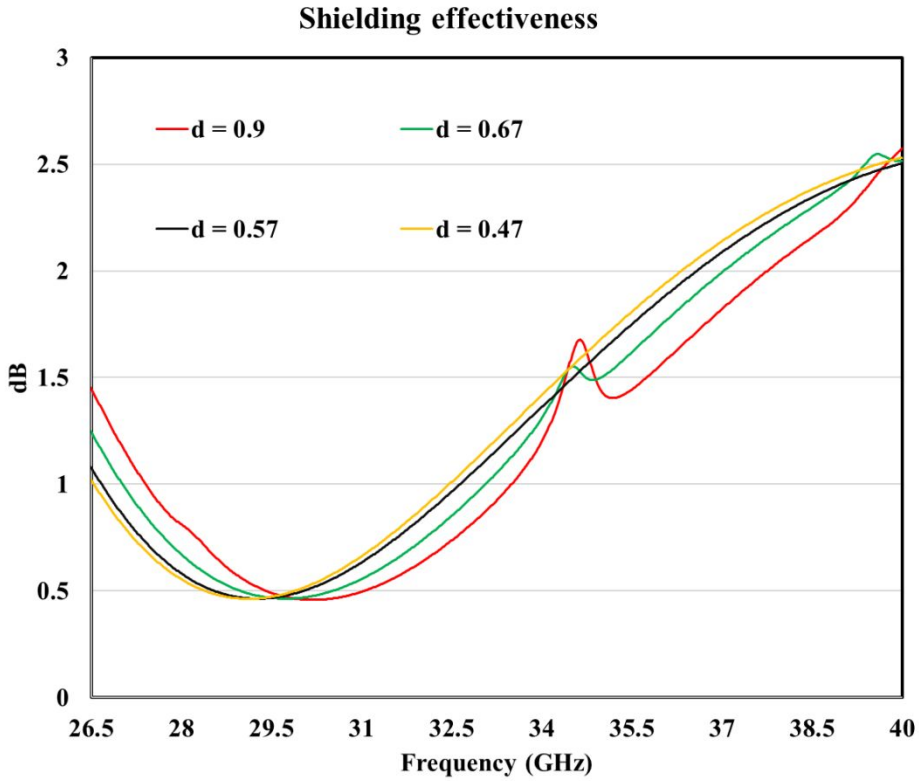


Fig. 4. SE (dB) of PU with different pore diameters (constant pore randomness and void fraction).

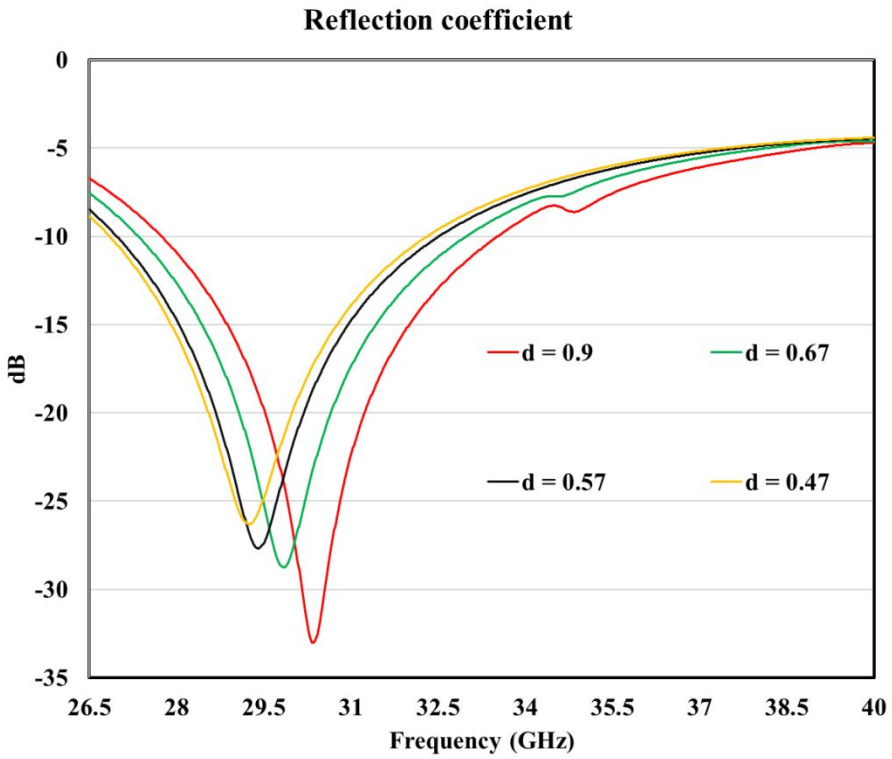


Fig. 5. S_{11} (dB) of PU with different pore diameters (constant pore randomness and void fraction).

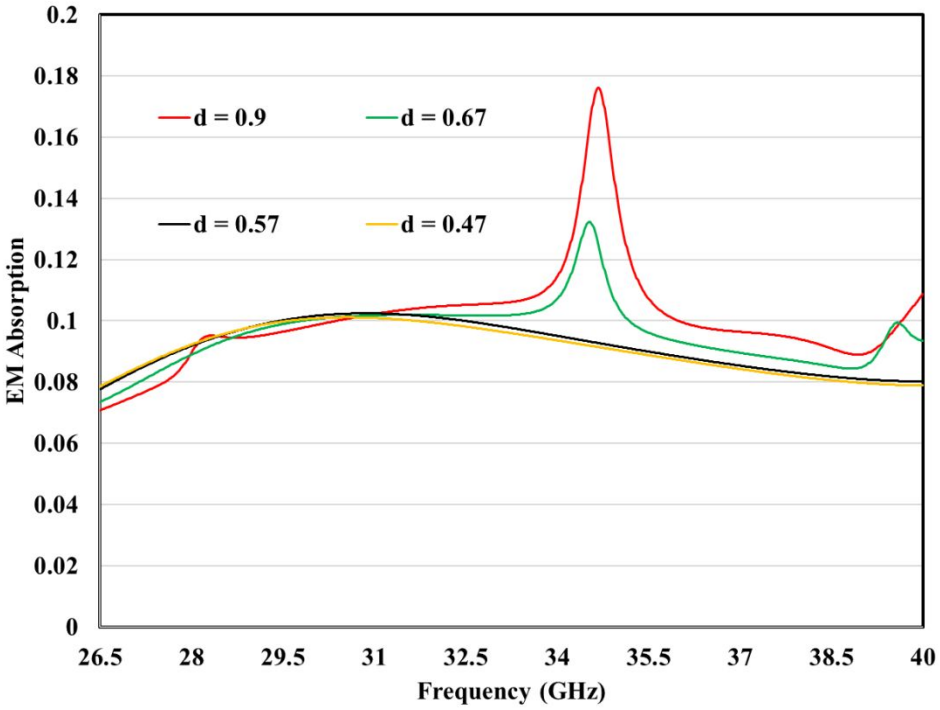


Fig. 6. EM absorption of PU with different pore diameters (constant pore randomness and void fraction).

TABLE I
RESONANCE FREQUENCY OF PU FOAM WITH DIFFERENT PORE DIAMETERS

Pore Diameter (mm)	Resonance Frequency (GHz)
0.47	29.24
0.57	29.42
0.67	29.84
0.9	30.35

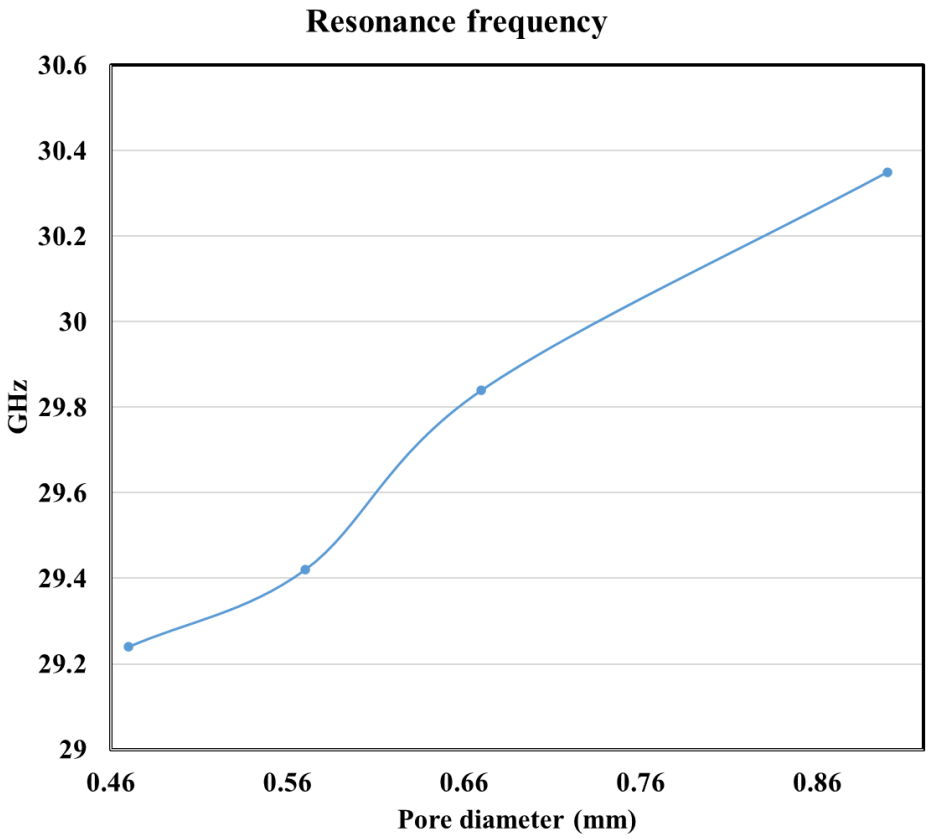


Fig. 7. Resonance frequency as a function of pore diameters (constant pore randomness and void fraction).

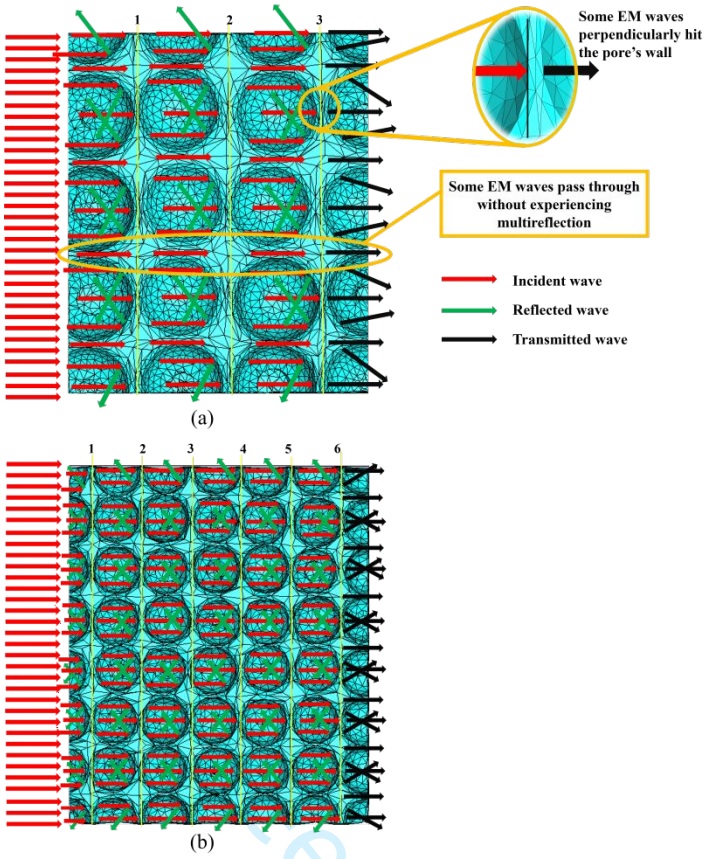


Fig. 8. EM waves and PU geometries interaction; (a): PU geometry with a pore diameter of 0.9 mm, (b): PU geometry with a pore diameter of 0.47 mm.

B. Pore Randomness

The pore randomness was manipulated using Blender software as described in Section II.B. The SE and S_{11} of PU foam geometries increased with increasing the pore randomness in the frequency range between resonance frequencies and 40 GHz as shown in Figs. 9 and 10, respectively. Such increments could be explained by the behavior of two coefficients: 1- Reflection coefficient: The EM waves tend to bounce off less of an ordered PU foam surface with zero randomness because many EM waves will perpendicularly pass through the geometry. In contrast, geometries with random surfaces reflect more EM waves due to higher multireflection in the first row of pores. 2- Transmission coefficient: Geometries with higher randomness factors have lower transmission coefficients (higher SE) because some EM waves experienced maximal interaction with the geometry. On the other hand, less interaction with the geometry occurred in geometries with lower R because some EM waves traveled through vacuum (dielectric constant = 1) more one than traveling through the geometry (dielectric constant = 6.55). As a result, geometries with lower R exhibited lower SE.

Apart from PU geometry with zero randomness, each geometry exhibited high EM absorption at a certain frequency as shown in Fig. 11. This trend could be because all geometries have the same void fraction which means they share the same effective permittivity. Each EM absorption peak (Fig. 11) corresponds to a minimum value of S_{11} (Fig. 10) and a maximum value of SE (Fig. 9) at the same time. This observation is consistent with equation (1). Additionally, it is worth noting that there were no EM absorption peaks at the resonance frequencies listed in Table II because the EM waves simultaneously experienced minimum reflection (S_{11}) and maximum transmission (minimum SE). Fig. 12 shows that the resonance frequency

increased with increasing the pore randomness from 0 to 0.2. Then, it started to gradually decrease as the randomness continued to rise.

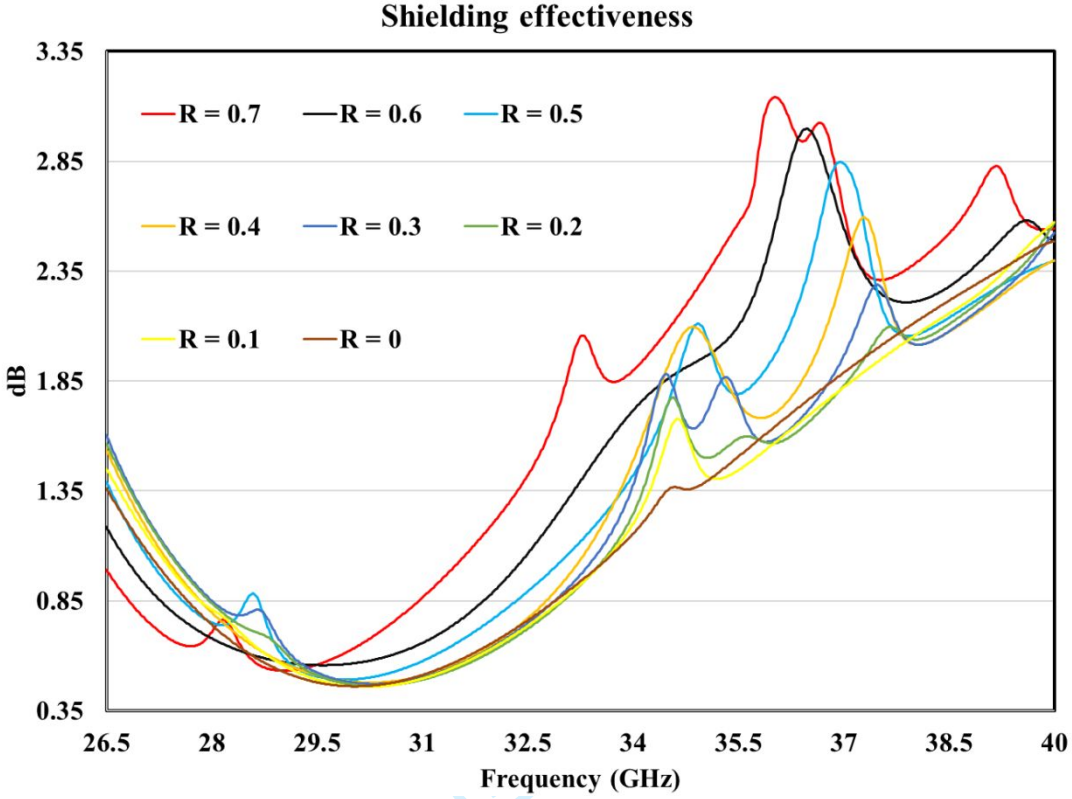


Fig. 9. SE (dB) of PU with different pore randomness (constant pore diameters and void fraction).

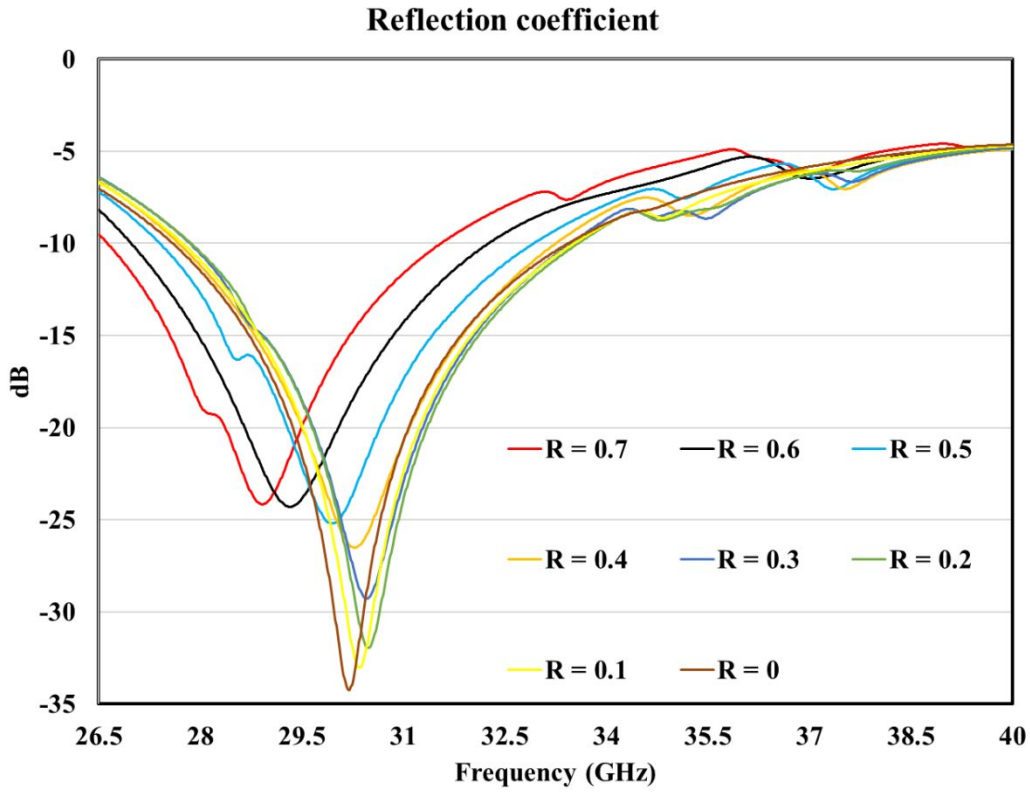


Fig. 10. S_{11} (dB) of PU with different pore randomness (constant pore diameters and void fraction).

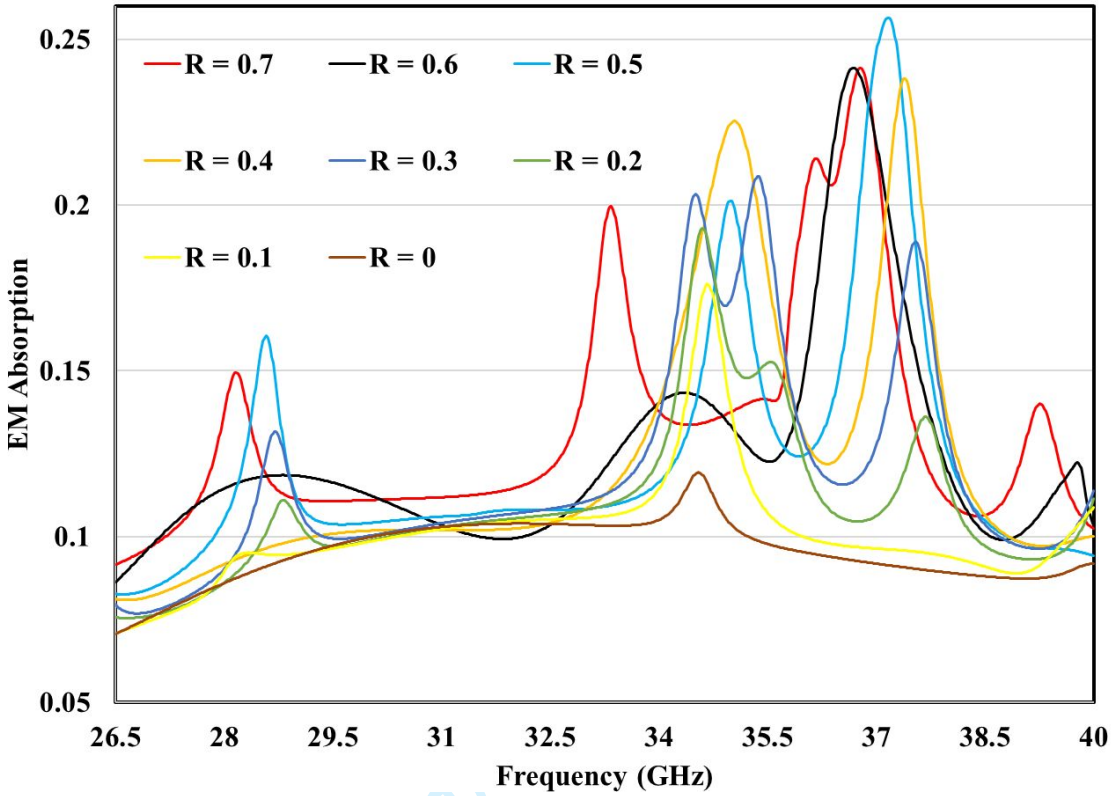


Fig. 11. EM absorption of PU with different pore randomness (constant pore diameters and void fraction).

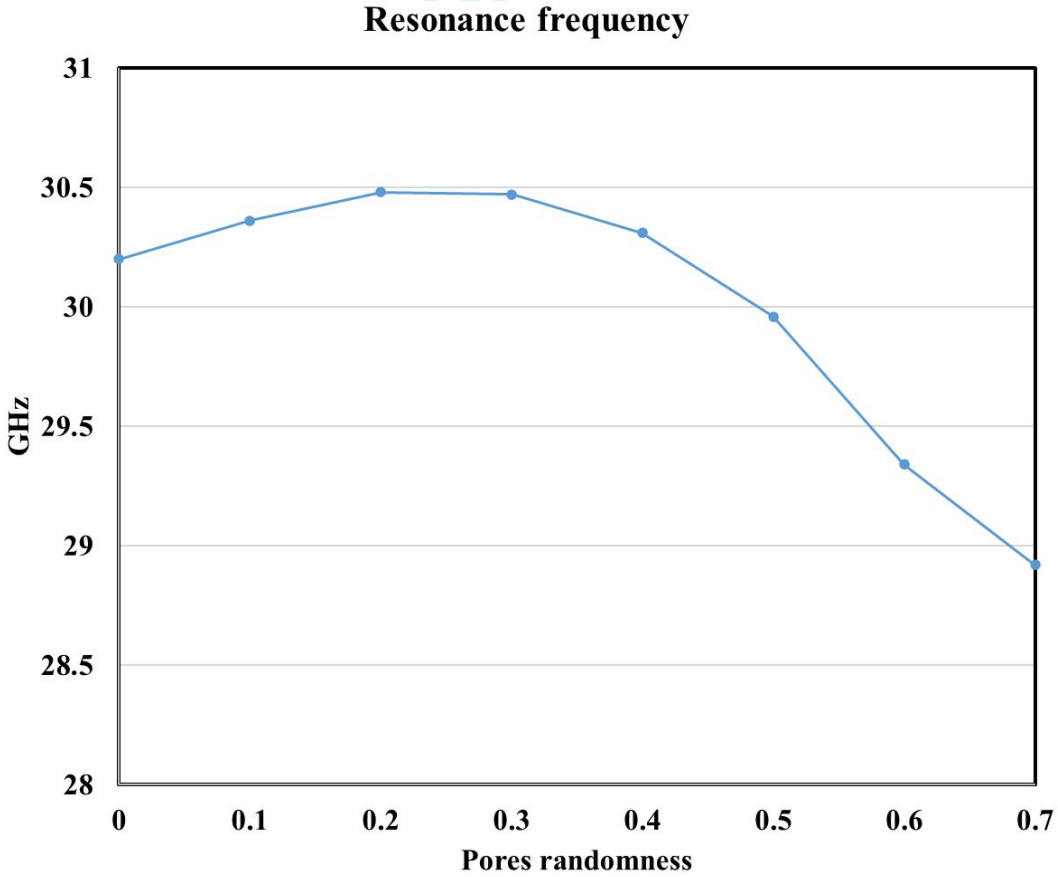


Fig. 12. Resonance frequency as a function of pore randomness (constant pore diameters and void fraction).

TABLE II
RESONANCE FREQUENCY OF PU FOAM WITH DIFFERENT PORE RANDOMNESS

Pore Randomness	Resonance Frequency (GHz)
0	30.20
0.1	30.36
0.2	30.48
0.3	30.47
0.4	30.31
0.5	29.96
0.6	29.34
0.7	28.92

C. Void Fraction

Fig. 13 shows that increasing the VF caused a decrease in the SE. The PU foam geometry of 0.5 VF generally showed the highest values of SE among all geometries. The reason for this trend is the relationship between S_{11} and VF. Decreasing the VF of PU foam geometries caused an increase in S_{11} as shown in Fig. 14. This behavior can be attributed to the increase in permittivity when decreasing the void fraction. Geometries with higher effective permittivity tend to reflect a higher amount of EM waves due to the increment in the impedance mismatching [53]. The increase in permittivity caused a decrease in the fr as listed in Table III. However, the fr of PU foam geometry with zero VF did not follow the same pattern in Fig. 14 because the EM waves did not experience any multiple reflections inside the geometry. Fig. 15 shows that some EM waves pass through the PU foam with minimal interaction inside the geometry when the VF is high, whereas the opposite manner occurred in geometries with low VF. Such interactions also could contribute to higher EM transmission (lower SE) in high VF geometries and lower EM transmission (higher SE) in low VF ones.

Fig. 13 also shows that the PU foam geometry with zero VF had the highest SE, in the 26.5 – 33 GHz frequency range, due to the high reflection which could occur because of the impedance mismatching induced by a higher permittivity in the absence of air (VF = 0). The SE decrement occurred in the 33 – 40 GHz frequency range could also be due to the impedance matching. The EM waves did not experience the multireflection phenomenon in this geometry due to the absence of pores, leading to lower EM absorption. Fig. 16 shows that EM absorption generally increased as the VF decreased, and the sample with 0.5 VF achieved the highest EM absorption at 34 GHz.

The relation between the resonance frequency and void fraction is presented in Fig. 17. The six datasets presented in Fig. 17 were used to establish the following empirical equation which expresses resonance frequency as a function of VF:

$$fr = 26.249\ VF + 13.008 \quad (7)$$

The R^2 value is 0.97 which also indicates a strong relationship between fr and VF.

For Peer Review

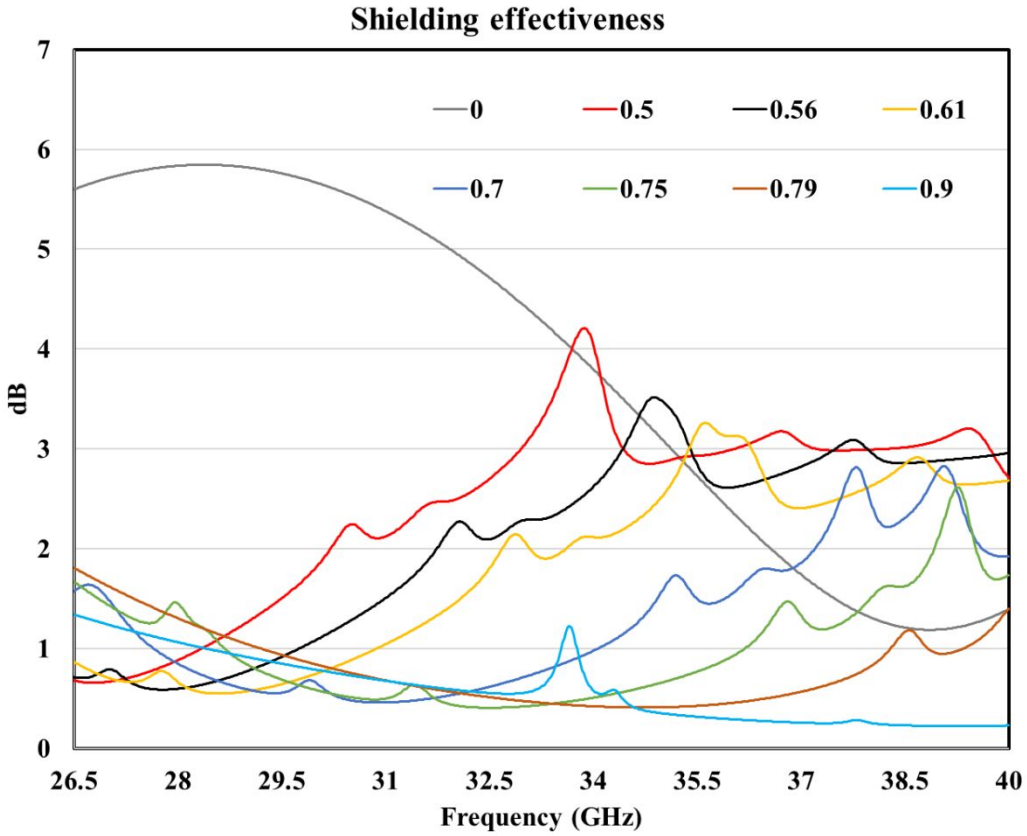


Fig. 13. SE (dB) of PU with different VF (constant pore diameters and randomness).

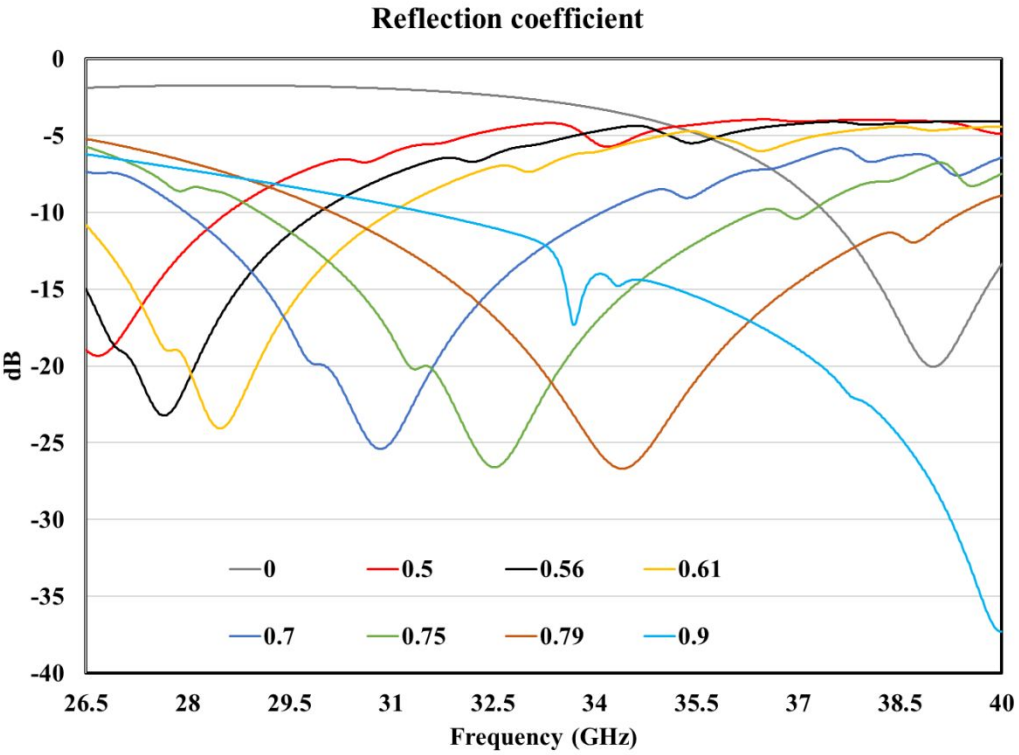


Fig. 14. S_{11} (dB) of PU with different VF (constant pore diameters and randomness).

TABLE III
RESONANCE FREQUENCY OF PU FOAM WITH DIFFERENT VOID FRACTIONS

Void Fraction	Resonance Frequency (GHz)
0	38.99
0.5	26.68
0.56	27.66
0.61	28.48
0.7	30.89
0.75	32.53
0.79	34.44

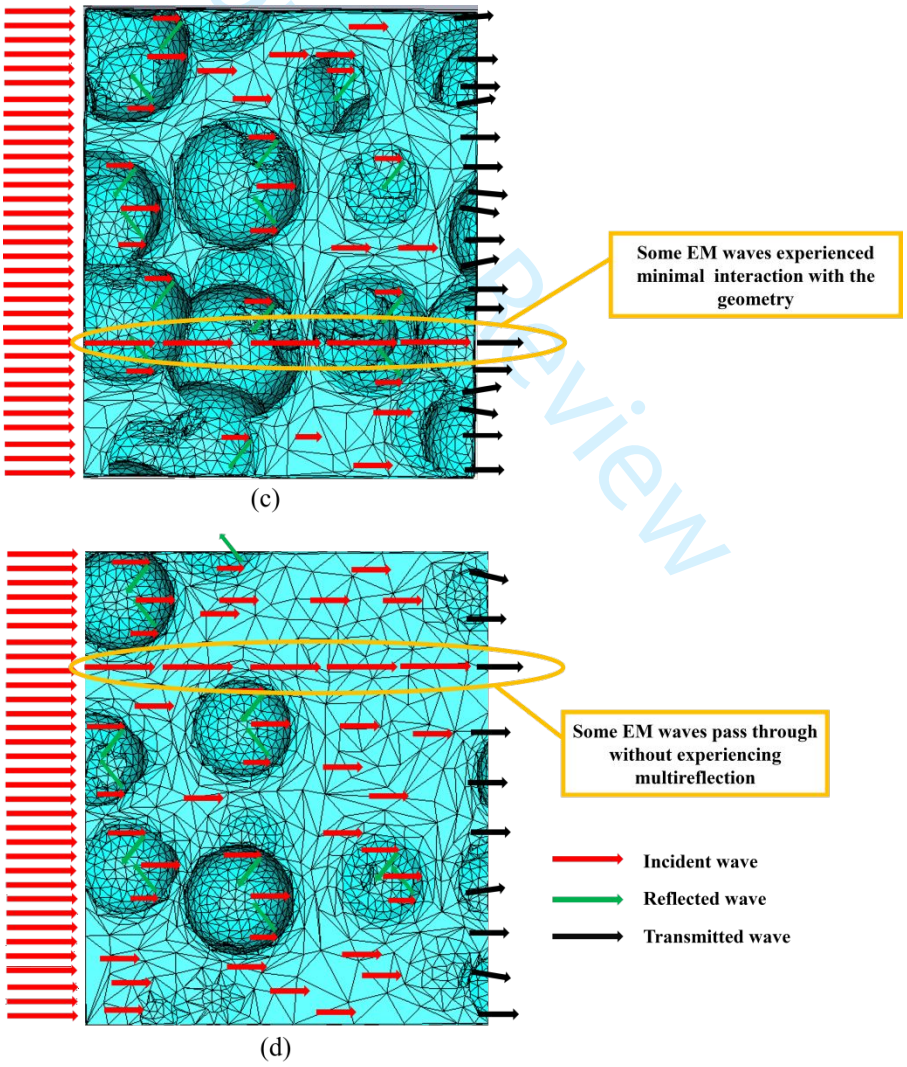


Fig. 15. EM waves and PU geometries interaction; (c): PU geometry with 0.79 VF, (d): PU geometry with 0.5 VF (constant pore diameters and randomness).

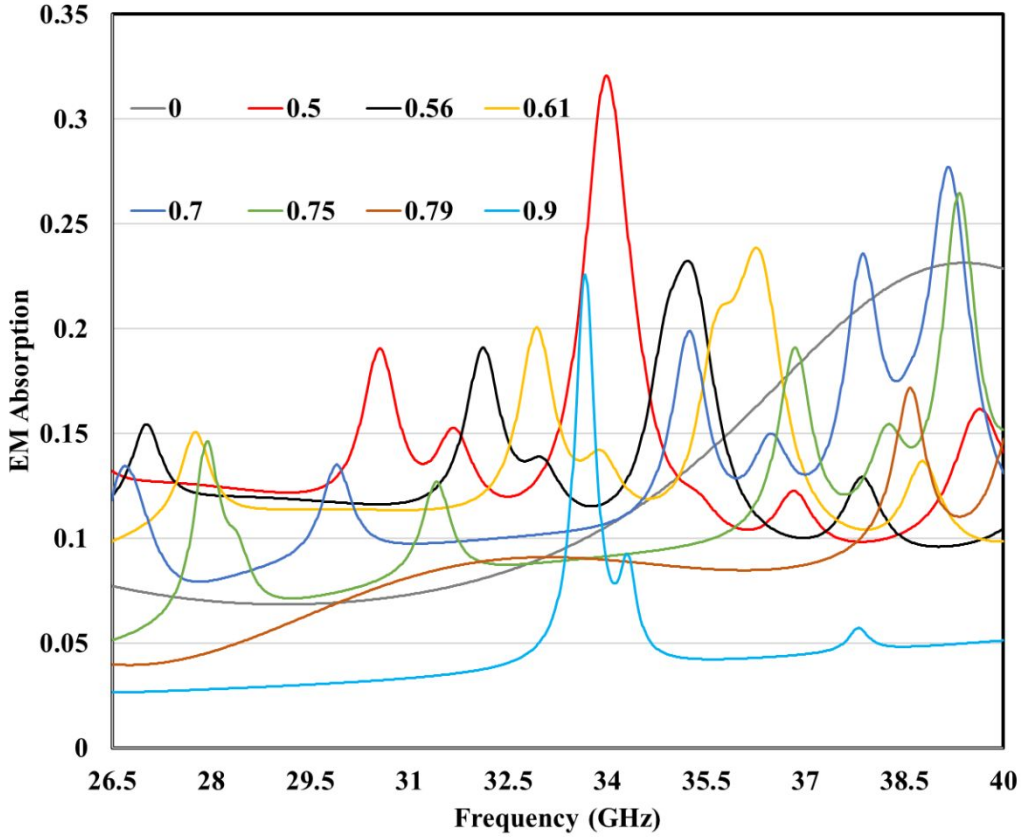


Fig. 16. EM absorption of PU with different VF (constant pore diameters and randomness).

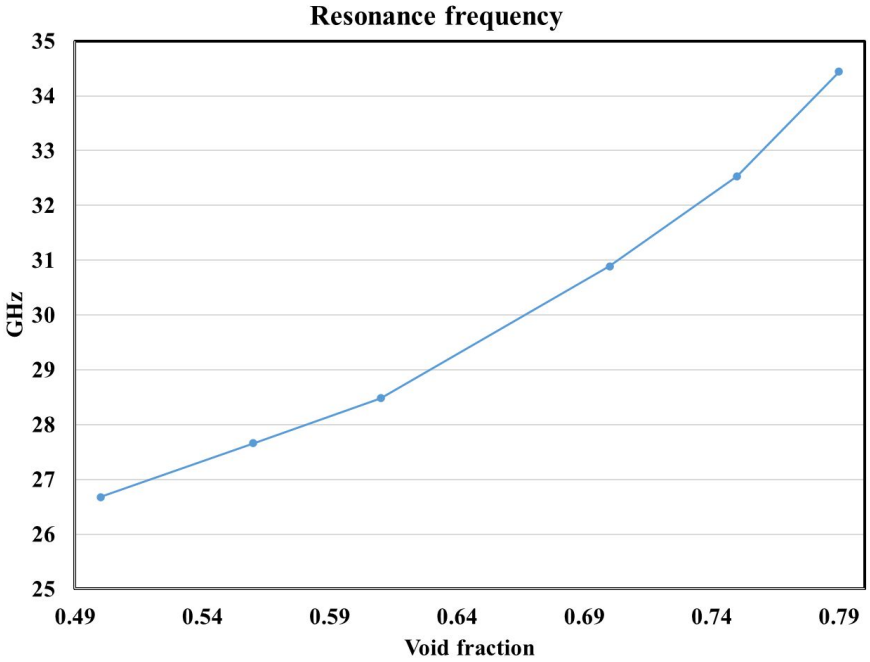


Fig. 17. Resonance frequency as a function of void fraction (constant pore diameters and randomness).

D. Validating CST Studio Simulation

Verifying the calculation's accuracy of CST Studio was conducted using two validations. These validations were performed on PTFE and PU foam with the dimensions of (15 cm ×10 cm ×1 cm) and (7.112 mm ×

3.556 mm × 3 mm), respectively. Fig. 18 shows the simulation and measurement setups for both samples. The first step was to measure the scattering parameters of each sample using an Anritsu vector network analyzer in the 26.5 – 40 GHz frequency range. The measurement was conducted based on placing the sample between the flanges of rectangular waveguide per the study conducted by Molenberg [54]. The Leica S6 D microscope was used to capture a high-resolution photo of the PU foam sample. Afterwards, ImageJ 1.53e software was employed to process the photo and determine the void fraction and average pore diameter, which were then used in Blender software to mimic the PU foam as presented in Fig. 19. The average values of pore diameter of PU foam geometry and real PU foam were 0.53 mm and 0.46 mm, respectively. The VF values of the PU foam geometry and real PU foam were 0.87 and 0.8, respectively. Finally, the two geometries were imported to CST Studio where the same measurement conditions were applied.

The comparison between the simulation and measurement results of PU foam and PTFE sample showed a good agreement as shown in Fig. 20. The PTFE sample exhibited better agreement compared to PU foam which can attributed to the complexity of PU foam geometry and the differences in pore diameters and void fraction.

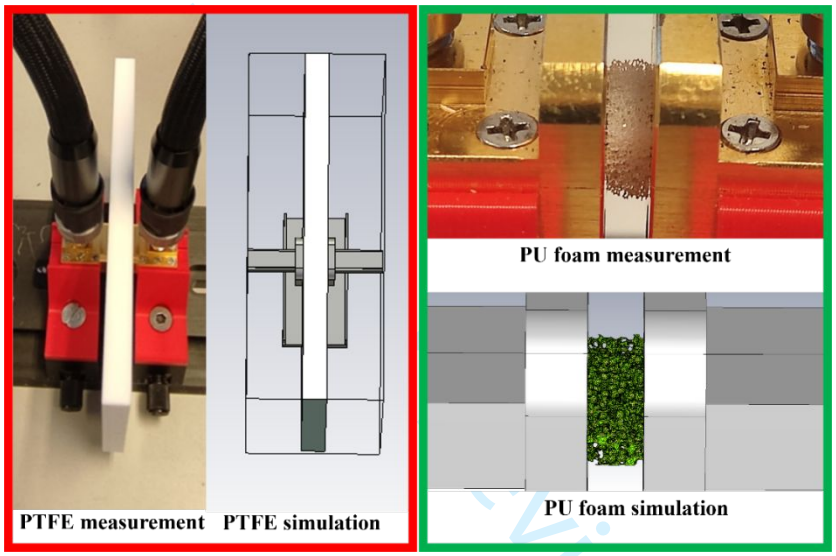


Fig. 18. Measurement and simulation setups.

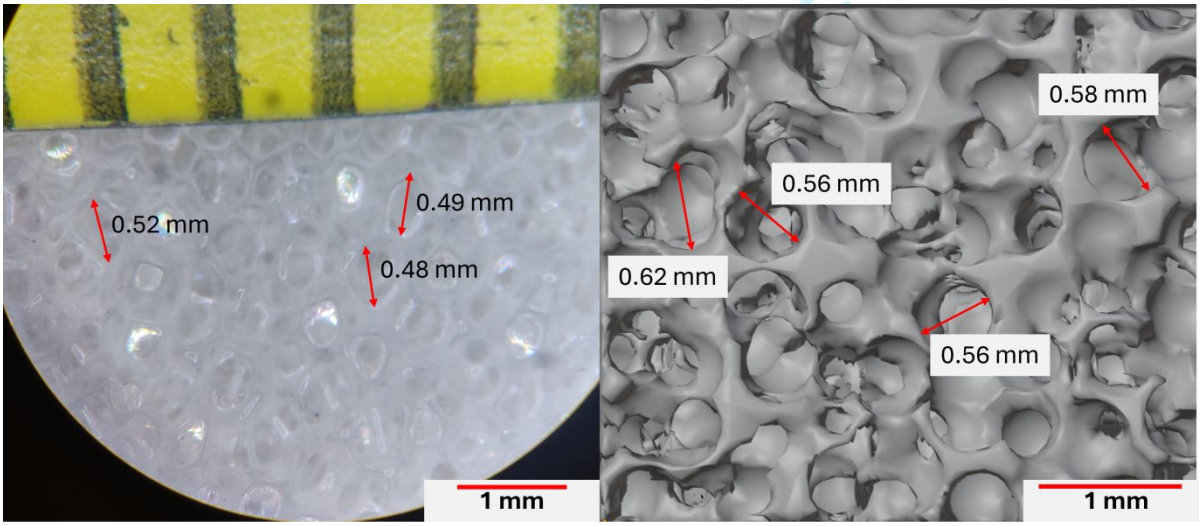


Fig. 19. Images of PU foam; (a): Real PU foam image captured using Leica S6 D microscope, (b): PU foam geometry constructed using Blender software.

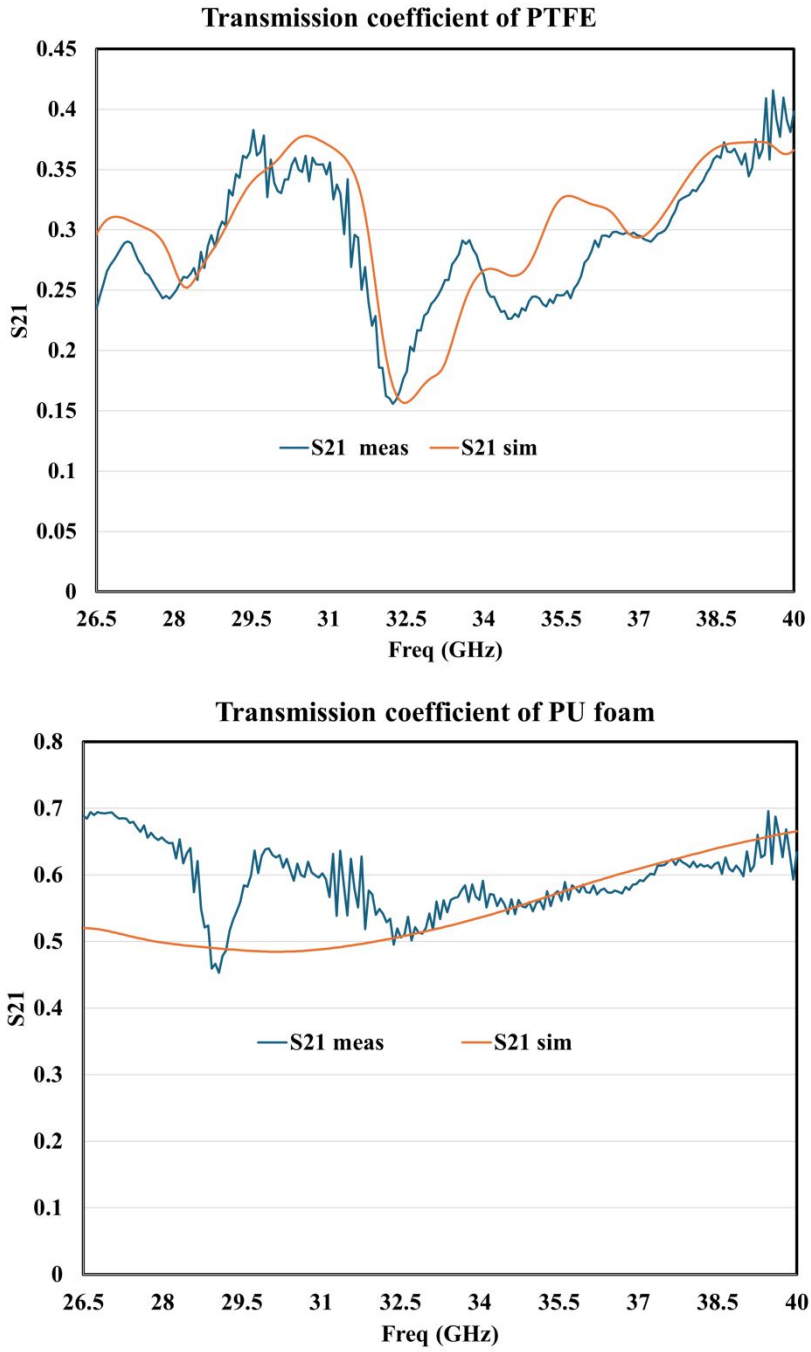


Fig. 20. The comparison of S_{21} obtained using CST Studio simulation and VNA measurement.

IV. CONCLUSION

The purpose of this study was to investigate the impact of pore diameters, pore randomness, and void fraction of PU foam on the electromagnetic shielding properties. Three different batches of PU foam geometries were constructed using Blender software. Then, CST Studio was used to simulate the scattering parameters of the geometries. It was found that the resonance frequency linearly increased with increasing the pore diameter and void fraction. The SE and S_{11} strongly correlate with void fraction, pore diameter, and randomness. This research can be reconducted in different frequency ranges and using different geometry shapes and parameters. For instance, CST Studio could be used to simulate PU foam geometries filled with conductive fillers before producing the prototypes, saving cost and time. Fabricating excellent EMI foam

shielding samples requires considering three studied factors.

ACKNOWLEDGMENT

The authors acknowledge the support of Benoît Hubert and Pascal Simon from the Welcome technological platform of UCLouvain for the measurement of the PU foam and PTFE samples. The work of I. Huynen as a research director is funded by the National Fund for Scientific Research (FNRS, Belgium). The authors also thank Blender foundation for making Blender software free and open source.

FUNDING

This work was performed in the frame of the UP_Plastics project co-funded by the European Union and the Walloon Region as part of the FEDER 2021-2027 Program.

REFERENCES

[1] V. Rathi, and V. Panwar, "Electromagnetic interference shielding analysis of conducting composites in near-and far-field region," *IEEE transactions on electromagnetic compatibility,* vol. 60, no. 6, pp. 1795-1801, 2018.

[2] V. Rathi, V. Panwar, G. Anoop, M. Chaturvedi, K. Sharma, and B. Prasad, "Flexible, thin composite film to enhance the electromagnetic compatibility of biomedical electronic devices," *IEEE Transactions on Electromagnetic Compatibility,* vol. 61, no. 4, pp. 1033-1041, 2018.

[3] B. Zhao, M. Hamidinejad, S. Wang, P. Bai, R. Che, R. Zhang, and C. B. Park, "Advances in electromagnetic shielding properties of composite foams," *Journal of Materials Chemistry A,* vol. 9, no. 14, pp. 8896-8949, 2021.

[4] L. Jin, Z. Haiyan, L. Ping, Y. Xijiang, and Z. Guoxun, "The electromagnetic shielding effectiveness of a low-cost and transparent stainless steel fiber/silicone resin composite," *IEEE Transactions on Electromagnetic Compatibility,* vol. 56, no. 2, pp. 328-334, 2013.

[5] J. V. Vas, and M. J. Thomas, "Electromagnetic shielding effectiveness of layered polymer nanocomposites," *IEEE Transactions on Electromagnetic Compatibility,* vol. 60, no. 2, pp. 376-384, 2017.

[6] B. Ratner, "The correlation coefficient: Its values range between+ 1/− 1, or do they?," *Journal of targeting, measurement and analysis for marketing,* vol. 17, no. 2, pp. 139-142, 2009.

[7] X. Zheng, H. Zhang, R. Jiang, Z. Liu, S. Zhu, W. Li, L. Jiang, and X. Zhou, "Lightweight polyurethane composite foam for electromagnetic interference shielding with high absorption characteristic," *Journal of Colloid and Interface Science,* vol. 649, pp. 279-289, 2023.

[8] H. Oraby, M. Darwish, M. H. Senna, and H. R. Tantawy, "Optimization of mechanical and electromagnetic interference shielding properties of expanded graphite/polyurethane composite foams," *SPE Polymers,* vol. 5, no. 3, pp. 331-342, 2024.

[9] M. Panahi-Sarmad, M. Noroozi, M. Abrisham, S. Eghbalinia, F. Teimoury, A. R. Bahramian, P. Dehghan, M. Sadri, and V. Goodarzi, "A comprehensive review on carbon-based polymer nanocomposite foams as electromagnetic interference shields and piezoresistive sensors," *ACS Applied Electronic Materials,* vol. 2, no. 8, pp. 2318-2350, 2020.

[10] S. Sultana, M. Rahaman, and M. R. Chandan, "Enhancing EMI Shielding Efficiency of Polyurethane Foam by Incorporating MWCNT-Decorated Hollow Glass Microspheres," *ACS omega*, 2025.

[11] J. M. Kim, Y. Lee, M. G. Jang, C. Han, and W. N. Kim, "Electrical conductivity and EMI shielding effectiveness of polyurethane foam–conductive filler composites," *Journal of Applied Polymer Science,* vol. 134, no. 5, 2017.

[12] B. Zhao, R. Wang, Y. Li, Y. Ren, X. Li, X. Guo, R. Zhang, and C. B. Park, "Dependence of electromagnetic interference shielding ability of conductive polymer composite foams with hydrophobic properties on cellular structure," *Journal of Materials Chemistry C,* vol. 8, no. 22, pp. 7401-7410, 2020.

[13] M. Wu, Q. Ren, P. Gao, W. Ma, B. Shen, L. Wang, W. Zheng, P. Cui, and X. Yi, "Enhanced electrical conductivity and EMI shielding performance through cell size-induced CNS alignment in PP/CNS foam," *Composites Communications,* vol. 43, pp. 101716, 2023.

[14] Z. Dai, Y. Wei, C. Hu, Z. Wang, A. Wei, W. Zhang, and X. Lin, "Effects of pore structure on wide-frequency electromagnetic interference shielding performance of carbonized wood," *Composites Communications,* vol. 38, pp. 101501, 2023.

[15] M. Antunes, "Recent trends in polymeric foams and porous structures for electromagnetic interference shielding applications," *Polymers,* vol. 16, no. 2, pp. 195, 2024.

[16] G. Wu, P. Xie, H. Yang, K. Dang, Y. Xu, M. Sain, L.-S. Turng, and W. Yang, "A review of thermoplastic polymer foams for functional applications," *Journal of Materials Science,* vol. 56, pp. 11579-11604, 2021.

For Peer Review

[17] S. Wang, Y. Huang, C. Zhao, E. Chang, A. Ameli, H. E. Naguib, and C. B. Park, "Theoretical modeling and experimental verification of percolation threshold with MWCNTs' rotation and translation around a growing bubble in conductive polymer composite foams," *Composites Science and Technology,* vol. 199, pp. 108345, 2020.
[18] L. Ma, M. Hamidinejad, L. Wei, B. Zhao, and C. B. Park, "Absorption-dominant EMI shielding polymer composite foams: Microstructure and geometry optimization," *Materials Today Physics,* vol. 30, pp. 100940, 2023.
[19] V. K. Selvaraj, and J. Subramanian, "A comparative study on bio-based PU foam reinforced with nanoparticles for EMI-shielding applications," *Polymers,* vol. 14, no. 16, pp. 3344, 2022.
[20] C. Afilipoaei, and H. Teodorescu-Draghicescu, "A review over electromagnetic shielding effectiveness of composite materials," in The 14th International Conference on Interdisciplinarity in Engineering—INTER-ENG, Târgu Mureș, Romania, 2020, pp. 23.
[21] I. A. Astuti, I. H. Purwanto, T. Hidayat, D. A. Satria, and R. Purnama, "Comparison of time, size and quality of 3d object rendering using render engine Eevee and cycles in blender," in 5th International Conference of Computer and Informatics Engineering (IC2IE), Jakarta, Indonesia, 2022, pp. 54-59.
[22] R. Abbas, U. ur Rehman, N. Sultan, U. Ghazanfar, T. Ali, and M. Nadeem, "3D printed lightweight honeycomb vent structures with subsequent coating of silver nanowires for efficient electromagnetic interference (EMI) shielding," *Heliyon,* vol. 10, no. 9, 2024.
[23] U. u. Rehman, A. Bilal, J. Faizan, A. Warsi, A. Ramzan, K. Shati, and M. Nadeem, "3D-Printed Pyramidal Honeycomb Structures Plated with Silver and Infused with Fe3O4–Epoxy Composite for Microwave Absorption Applications," *Advanced Engineering Materials,* vol. 27, no. 2, pp. 2402030, 2025.
[24] K. Emori, S. Fushimi, T. Miura, and A. Yonezu, "FEM simulation of polymeric foam with random pore structure: Uniaxial compression with loading rate effect," *Polymer testing,* vol. 82, pp. 106303, 2020.
[25] N. Contuzzi, S. L. Campanelli, F. Caiazzo, and V. Alfieri, "Design and fabrication of random metal foam structures for laser powder bed fusion," *Materials,* vol. 12, no. 8, pp. 1301, 2019.
[26] W. Sun, X. Ren, J. Zhang, and H. Xu, "Numerical Simulation of Crack Propagation in Rocks with Random Pores Based on Improved Smoothed Particle Hydrodynamics Method," *Applied Sciences,* vol. 15, no. 4, pp. 1826, 2025.
[27] N. Hu, F. Deng, W. Xu, Y. Deng, J. Yang, J. Zhang, and R. Yang, "Random Foam Meso-Model and Mechanical Properties of Foam Concrete," *Strength of Materials,* vol. 55, no. 5, pp. 1079-1088, 2023.
[28] M. M. Mezedur, M. Kaviany, and W. Moore, "Effect of pore structure, randomness and size on effective mass diffusivity," *AIChE journal,* vol. 48, no. 1, pp. 15-24, 2002.
[29] W. Wang, A. C. Y. Yuen, H. Long, W. Yang, A. Li, L. Song, Y. Hu, and G. H. Yeoh, "Random nano-structuring of PVA/MXene membranes for outstanding flammability resistance and electromagnetic interference shielding performances," *Composites Part B: Engineering,* vol. 224, pp. 109174, 2021.
[30] E. Agostini, G. Boccardo, and D. Marchisio, "An open-source workflow for open-cell foams modelling: Geometry generation and CFD simulations for momentum and mass transport," *Chemical Engineering Science,* vol. 255, pp. 117583, 2022.
[31] S. J. Franson, and R. W. Ziolkowski, "Gigabit per second data transfer in high-gain metamaterial structures at 60 GHz," *IEEE Trans Antennas Propag,* vol. 57, no. 10, pp. 2913-2925, 2009.
[32] W. Zheng, B. Liu, C. Yang, and A. Zhang, "Optimal design of 3D macro-structures for multi-layer foams achieving ultra-broadband microwave absorption properties and high retention after immersion in brine," *Composites Part B: Engineering,* vol. 268, pp. 111094, 2024.
[33] W. Gu, S. J. H. Ong, Y. Shen, W. Guo, Y. Fang, G. Ji, and Z. J. Xu, "A lightweight, elastic, and thermally insulating stealth foam with high infrared-radar compatibility," *Advanced Science,* vol. 9, no. 35, pp. 2204165, 2022.
[34] Z. Yang, X. Sun, J. Tian, H. Li, H. Yu, H. Wang, M. Zhou, and Q. Huang, "Broadband and polarization-insensitive microwave absorbing composite material with transmission performance based on indium tin oxide metamaterial," *Journal of Materials Science: Materials in Electronics,* vol. 31, no. 16, pp. 13838-13844, 2020.
[35] O. Losito, D. Barletta, and V. Dimiccoli, "A wide-frequency model of metal foam for shielding applications," *IEEE Transactions on Electromagnetic Compatibility,* vol. 52, no. 1, pp. 75-81, 2010.
[36] J. Tahalyani, M. J. Akhtar, and K. K. Kar, "Heterolayered composite of carbon nanofibers sandwiched between poly (ethylene terephthalate) and polyurethane for flexible electromagnetic shielding application," *ACS Applied Nano Materials,* vol. 4, no. 11, pp. 12146-12157, 2021.
[37] Z. Sun, L. Yan, C. Wang, X. Zhao, and R. X.-K. Gao, "An FSS-Based Broadband Absorber for Electromagnetic Shielding," in Asia-Pacific International Symposium on Electromagnetic Compatibility (APEMC), Beijing, China, 2022, pp. 675-677.
[38] W. Yang, H. Maozhen, Z. Payzulla, S. Yangxin, T. Jing, and L. Qi, "Structural Design and Simulation of a High Performance Electromagnetic Shielding Cabinet Door," in IEEE 9th International Symposium on Microwave, Antenna, Propagation and EMC Technologies for Wireless Communications (MAPE), Chengdu, China, 2022, pp. 357-360.
[39] J. N. C. Hernandez, G. Link, S. Soldatov, A. Füssel, M. Schubert, and U. Hampel, "Experimental and numerical analysis of the complex permittivity of open-cell ceramic foams," *Ceramics International,* vol. 46, no. 17, pp. 26829-26840, 2020.
[40] A. Genç, H. Doğan, L. Turhan, A. Kocakuşak, and S. Helhel, "Investigation of the radiated emission of honeycomb structured aluminum foam/cellular heatsinks at 1–10 GHz," *Materials Chemistry and Physics,* vol. 324, pp. 129614, 2024.

For Peer Review

[41] D. Wang, J. Li, L. Zheng, X. Sun, M. Sun, C. Wang, Z. Bi, B. Zhou, L. Wang, and Q. Li, "Lightweight thermoplastic polyurethane/multi-wall carbon nanotube foams with a continuous gradient cell structure for electromagnetic interference shielding," *Energy,* vol. 304, pp. 131864, 2024.
[42] H. Breiss, A. El Assal, R. Benzerga, A. Harmouch, A. Jrad, and A. Sharaiha, "Design and characterization of a lightweight and flexible carbon fiber-loaded silicone foam-based broadband metamaterial absorber for microwave applications," *Mater Res Bull,* vol. 176, pp. 112791, 2024.
[43] Y. Liu, A. Thakur, B. Anasori, and S. Mohammadi, "Ka-band EMI Shielding Effectiveness of Ti 3 C 2 T x MXene," in IEEE/MTT-S International Microwave Symposium-IMS San Diego, CA, USA, 2023, pp. 760-762.
[44] F. Al-Janabi, M. J. Singh, and A. P. S. Pharwaha, "Development of Microstrip Antenna for Satellite Application at Ku/Ka Band," *J. Commun.,* vol. 16, no. 4, pp. 118-125, 2021.
[45] A. Akdagli, and K. Guney, "New wide-aperture-dimension formula obtained by using a particle swarm optimization for optimum gain pyramidal horns," *Microwave and Optical Technology Letters,* vol. 48, no. 6, pp. 1201-1205, 2006.
[46] X. Liang, Y. Shen, Y. Liu, J. Wang, Y. Gao, S. Li, M. Wang, and S. Gao, "Investigations on the basic electrical properties of Polyurethane foam material," in IEEE 11th International Conference on the Properties and Applications of Dielectric Materials (ICPADM), Sydney, NSW, Australia, 2015, pp. 863-866.
[47] M. Bai, M. Poulsen, and S. Ducharme, "Effects of annealing conditions on ferroelectric nanomesa self-assembly," *Journal of Physics: Condensed Matter,* vol. 18, no. 31, pp. 7383, 2006.
[48] L. Márquez-Torres, J. Ochoa-Pineda, P. Pico, J. P. Valdés, D. Becerra, A. Pinilla, E. Pereyra, and N. Ratkovich, "Comparison of 63 different void fraction correlations for different flow patterns, pipe inclinations, and liquid viscosities," *SN Applied Sciences,* vol. 2, pp. 1-24, 2020.
[49] G. Saxena, N. K. Devbanshi, M. Srivastava, and N. K. Yadav, "High Q and High EMR Hepta Band Single Layer Metasurface Absorber for EMI and Sensing Applications in C, X, Ku, K and Ka Band," in IEEE Wireless Antenna and Microwave Symposium (WAMS), Rourkela, India, 2022, pp. 1-5.
[50] C. Retailleau, J. A. Eddine, F. Ndagijimana, F. Haddad, B. Bayard, B. Sauviac, P. Alcouffe, M. Fumagalli, V. Bounor-Legaré, and A. Serghei, "Universal behavior for electromagnetic interference shielding effectiveness of polymer based composite materials," *Composites Science and Technology,* vol. 221, pp. 109351, 2022.
[51] A. Kocakusak, A. Genc, H. Dogan, L. Turhan, and S. Helhel, "Electromagnetic Interference Shielding Effectiveness Performance of Various Aluminum Foam/Cellular Structures at C-Band: A Numerical and Experimental Investigation," *Advanced Engineering Materials*, pp. 2500933, 2025.
[52] Y. Zhang, Y. Wu, J. Yan, and W. Wang, "Wideband high-selectivity filtering all-frequency absorptive power divider with deep out-of-band suppression," *IEEE Transactions on Plasma Science,* vol. 49, no. 7, pp. 2099-2106, 2021.
[53] Y.-N. Gao, Y. Wang, T.-N. Yue, and M. Wang, "Achieving absorption-type electromagnetic shielding performance in silver micro-tubes/barium Ferrites/Poly (lactic acid) composites via enhancing impedance matching and electric-magnetic synergism," *Composites Part B: Engineering,* vol. 249, pp. 110402, 2023.
[54] I. Molenberg, M. M. Bernal, P. Bollen, D. Spote, R. Verdejo, T. Pardoen, C. Bailly, and I. Huynen, "Simple, convenient, and nondestructive electromagnetic characterization technique for composite and multiscale hybrid samples at microwave frequencies," *Microwave and Optical Technology Letters,* vol. 56, no. 2, pp. 504-509, 2014.

For Peer Review